

A EUROPEAN JOURNAL OF CHEMICAL BIOLOGY

# CHEM **BIO** CHEM

SYNTHETIC BIOLOGY & BIO-NANOTECHNOLOGY

## Accepted Article

Title: An Fc-Small Molecule Conjugate for Targeted Inhibition of the Adenosine 2A Receptor

Authors: Po-Yuan Hsiao; Jay Kalin; Im-Hong Sun; Mohammed Amin; Ying-Chun Lo; Meng-Jung Chiang; John Giddens; Polina Sysa-Shah; Kathleen Gabrielson; Lai-Xi Wang; Jonathan Powell; Philip A. Cole

This manuscript has been accepted after peer review and the authors have elected to post their Accepted Article online prior to editing, proofing, and formal publication of the final Version of Record (VoR). This work is currently citable by using the Digital Object Identifier (DOI) given below. The VoR will be published online in Early View as soon as possible and may be different to this Accepted Article as a result of editing. Readers should obtain the VoR from the journal website shown below when it is published to ensure accuracy of information. The authors are responsible for the content of this Accepted Article.

To be cited as: ChemBioChem 10.1002/cbic.201600337

Link to VoR: <http://dx.doi.org/10.1002/cbic.201600337>

A Journal of



[www.chembiochem.org](http://www.chembiochem.org)

WILEY-VCH

## An Fc-Small Molecule Conjugate for Targeted Inhibition of the Adenosine 2A Receptor

Po-Yuan Hsiao<sup>[a]</sup>, Jay H. Kalin<sup>[a]</sup>, Im-Hong Sun<sup>[b]</sup>, Mohammed N. Amin<sup>[c], [d]</sup>, Ying-Chun Lo<sup>[b], [e]</sup>, Meng-Jung Chiang<sup>[a], [f]</sup>, John Giddens<sup>[c]</sup>, Polina Sysa-Shah<sup>[g]</sup>, Kathleen Gabrielson<sup>[h]</sup>, Lai-Xi Wang<sup>[c]</sup>, Jonathan D. Powell<sup>[b]</sup>, Philip A. Cole<sup>[a], \*</sup>

- 
- [a] P.Y. Hsiao, Dr. J. H. Kalin, Dr. M. J. Chiang, Prof. Dr. P. A. Cole  
Department of Pharmacology and Molecular Sciences,  
Johns Hopkins University School of Medicine, Baltimore, MD 21205, U.S.A.  
E-mail: pcole1@jhmi.edu
- [b] I. H. Sun, Dr. Y. C. Lo, Prof. Dr. J. D. Powell  
Sidney-Kimmel Comprehensive Cancer Research Center,  
Department of Oncology,  
Johns Hopkins School of Medicine, Baltimore, MD 21205, U.S.A.
- [c] Dr. M. N. Amin, J. Giddens, Prof. Dr. L. X. Wang  
Department of Chemistry and Biochemistry,  
University of Maryland, College Park, MD 20742, U.S.A.
- [d] Dr. M. N. Amin  
Center for Vaccine Development,  
University of Maryland School of Medicine, Baltimore, MD 21201, U.S.A.
- [e] Dr. Y. C. Lo  
Department of Pathology,  
Yale School of Medicine, New Haven, CT 06510, U.S.A.
- [f] Dr. M. J. Chiang  
Division of Viral Products, Office of Vaccines Research and Review,  
Center for Biologics Evaluation and Research,  
U.S. Food and Drug Administration, Silver Spring, MD 20993, U.S.A.
- [g] Dr. P. Sysa-Shah  
Russell H. Morgan Department of Radiology and Radiological Science,  
Johns Hopkins University, Baltimore, MD 21205, U.S.A.
- [h] Prof. Dr. K. Gabrielson  
Department of Molecular and Comparative Pathobiology,  
Johns Hopkins School of Medicine, Baltimore, MD 21205, U.S.A.

### Abstract

The adenosine A<sub>2A</sub> receptor (A<sub>2A</sub>R) is expressed in immune cells as well as heart and lung tissue and has been intensively studied as a therapeutic target for multiple disease indications. Inhibitors of the A<sub>2A</sub>R have the potential for stimulating immune response which could be valuable for cancer immune surveillance and mounting a response against pathogens. One well-established potent and selective small-molecule A<sub>2A</sub>R antagonist, ZM-241385 (ZM), has a short pharmacokinetic half-life and has the potential for systemic toxicity due to A<sub>2A</sub>R effects in the brain and the heart. In this study, we designed an analog of ZM for tethering to the Fc domain of the immunoglobulin IgG3 using expressed protein ligation. The resulting protein-small molecule conjugate, Fc-ZM, retained high affinity for both the FcγRI and the neonatal Fc receptor (FcRn). In addition, Fc-ZM was a potent A<sub>2A</sub>R antagonist as measured in a cell-based cAMP assay. Cell-based assays also revealed that

Fc-ZM could stimulate interferon  $\gamma$  production in splenocytes in a fashion that was dependent on the presence of A<sub>2A</sub>R. We found that Fc-ZM compared with the small molecule ZM was a superior A<sub>2A</sub>R antagonist in mice, consistent with the possibility that Fc attachment can improve pharmacokinetic and/or pharmacodynamic properties of the small molecule.

## Keywords

Antibodies. Drug design, Immunology, Inflammation, Inhibitors. Protein design, Protein modification.

## Introduction

A<sub>2A</sub>R is one of four adenosine receptor subtypes and is a G-protein coupled receptor (GPCR) that is expressed in immune cells as well as brain and heart<sup>[1]</sup>. A<sub>2A</sub>R agonists such as CGS21680 (CGS) have been explored as immunosuppressive agents but also have been used in human clinical studies to assess cardiac function<sup>[2]</sup>. A<sub>2A</sub>R antagonists like ZM-241385 (ZM) have been investigated as immunostimulatory agents and have also been studied as treatments for neurologic disease<sup>[3]</sup>. There have been two principle challenges with developing A<sub>2A</sub>R modulators as therapeutics. The first is that many A<sub>2A</sub>R ligands have very short pharmacokinetic half-lives, which makes delivery of a consistent dose difficult<sup>[2, 4]</sup>. The second is that A<sub>2A</sub>R ligands would be expected to affect physiology in multiple organs because of the diverse distribution of the A<sub>2A</sub> receptors<sup>[1]</sup>.

Previously, our group attempted to address both of these challenges by tethering the A<sub>2A</sub>R agonist CGS to the Fc domain of an immunoglobulin<sup>[5]</sup>. The antibody Fc domain is the key component in many biologics that confers a very long half-life, several days to weeks, allowing for infrequent dosing<sup>[6]</sup>. The accepted basis for such a long half-life is the Fc's interactions with the neonatal receptor (FcRn) which facilitates recycling of the Fc-containing molecules into the circulation rather than lysosomal removal<sup>[7]</sup>. Another isoform of the Fc receptor, Fc $\gamma$ RI, which is commonly expressed on antigen presenting cells, can allow for localization of Fc-containing molecules in sites of high immunoactivation through multiple receptor engagements on the same cell, such as myeloid cells, or neighboring immune cells like T cells and antigen presenting cells<sup>[8]</sup>. Fc fusion has been used in a variety of protein fusion drugs that are clinically approved including etanercept, which targets the TNF $\alpha$  receptor and is used for rheumatoid arthritis and other immune disorders<sup>[9]</sup>. Previously we adapted a semisynthetic method, expressed protein ligation<sup>[10]</sup>, to attach the Fc domain to the small molecule CGS. We showed that Fc-CGS indeed had a multi-day half-life in mice and was much more potent at treating autoimmune pneumonitis than the small molecule CGS<sup>[5]</sup>.

Here we explore the pharmacologic potential of linking an A<sub>2A</sub>R antagonist ZM to the

IgG3 Fc domain. Originally developed by the Zeneca group for neuroprotection and treatment of cognitive disorders, ZM selectively and potently inhibits the human A<sub>2A</sub>R with a K<sub>i</sub> of 0.8 nM<sup>[2]</sup>. However, ZM was also reported to have a short pharmacokinetic half-life (less than 20 min in cats), whether administered orally or intravenously<sup>[11]</sup>, with no detectable levels present in plasma 4 h after oral administration. Fc attachment could enhance its stability by the FcRn recycling mechanism as well as by preventing hepatic metabolism by prohibiting uptake in hepatocytes. Below we discuss our synthetic efforts toward Fc-ZM and its initial pharmacologic characterization.

## Results and Discussions

### Synthesis of Fc-ZM.

In designing Fc-ZM, we considered the key structural features required for antagonistic activity and ensured that the derivatization of the ZM small molecule would preserve its potency for binding and inhibition. We thus pursued the chemical synthesis of A-ZM (Scheme 1), a form of ZM in which the phenol would be derivatized with a carboxylic acid that could be convenient for connecting a synthetic linker. Prior X-ray crystallographic studies of ZM in complex with the A<sub>2A</sub>R revealed that the phenol was relatively solvent exposed<sup>[12]</sup>. We thus predicted that A-ZM would retain the pharmacodynamic properties of the parent compound ZM. The synthesis of A-ZM began with commercially available 4-hydroxybenzoxonitrile **1** which was alkylated with *t*-butyl bromoacetate to generate intermediate **2**. At the same time, the sulfone building block, intermediate **6**, was prepared according to previously published procedures<sup>[13]</sup>. Briefly, the commercially available 2-furonitrile starting material **3** was cyclized with aminoguanidine to generate aminotriazole **4**. Condensation of **4** with *N*-cyanodithioiminocarbonate provided heterocyclic thioether **5** which was subsequently oxidized with mCPBA to yield sulfone intermediate **6**. With the two building blocks **2** and **6** in hand, A-ZM was generated by first hydrogenating intermediate **2** to afford phenethylamine **7**. Nucleophilic displacement of the sulfone with the resulting primary amine and subsequent base-catalyzed removal of the *t*-butyl group provided the desired compound in seven overall steps. Separately, we prepared an ethylene-oxy linker terminating in a Cys residue by solid phase synthesis for use in expressed protein ligation. The size of this linker was projected to be of sufficient length, about 100 angstroms in extended conformation, to allow for dual engagement of the ZM component with the A<sub>2A</sub>R and the Fc domain with Fc receptors present on different cell types<sup>[5]</sup>. Consistent with our previously reported Fc-CGS conjugate, we prepared C-ZM to be used in the subsequent ligation reaction (Scheme 2).

With C-ZM in hand, it was ligated to the Fc protein via expressed protein ligation. In order to produce Fc in its glycosylated, disulfide-linked form, we expressed an

Fc-intein-chitin binding domain (CBD) construct containing the mouse IgG3 Fc domain (Fig. 1) in Sf9 insect cells via the baculovirus expression system as previously described<sup>[5, 14]</sup>. The secreted Fc-intein-CBD was isolated, purified with chitin resin, and treated with sodium 2-mercaptoethanesulfonate (MESNA) to form the free Fc thioester. The Fc thioester was then reacted with C-ZM or cysteine to make Fc-ZM and Fc, respectively. We chose expressed protein ligation to ensure chemoselectivity at the C-terminus of the Fc protein due to its technical simplicity and high yield in comparison with other methods. SDS-PAGE revealed Fc and Fc-ZM with more than 90% purity based on Coomassie staining (Fig. 2A). Note that the broad banding can be understood to be related to heterogenous Fc glycosylation as analyzed previously<sup>[15]</sup>. High-resolution LC-MS confirmed the expected mass after deglycosylation by PNGase F (Fig. 2B).

### Binding to the A<sub>2A</sub>R.

To explore the potential of Fc-ZM to bind and antagonize the A<sub>2A</sub>R, we treated wild-type mouse splenocytes with Fc-ZM and control compounds for 1 hour and measured the subsequent production of cyclic AMP (cAMP), a known second messenger generated in response to A<sub>2A</sub>R activation<sup>[15]</sup>. The treatments were either done alone (Fig. 3A) or in combination with the A<sub>2A</sub>R agonist CGS (Fig. 3B and 3C), to assess receptor antagonism. We chose a high dose (1 μM) and a more moderate dose (250 nM) of the ZM compounds to get an approximate understanding of their potency. Importantly, the mouse splenocytes were pre-activated with 2 μg/ml of anti-CD3 and anti-CD28 to enhance A<sub>2A</sub>R expression on the cell surface. As expected with A<sub>2A</sub>R activation, CGS treatment led to a sharp increase in intracellular cAMP production. Treatments with ZM, A-ZM, C-ZM, or Fc demonstrated no changes in cAMP levels. On the other hand, when treated in combination with CGS, Fc-ZM and its ZM-containing precursors inhibited the production of cAMP in a potent manner. Notably, Fc-alone does not affect cAMP production induced by CGS, indicating that the antagonism by Fc-ZM is due to a functional ZM moiety that is able to bind and inhibit A<sub>2A</sub>R activation.

While the antagonist effects of Fc-ZM appear to have been slightly smaller than that of A-ZM and perhaps some of the other ZM analogs at these concentrations, there could be several reasons for this. It is possible that Fc-ZM has reduced affinity for A<sub>2A</sub>R relative to that of A-ZM and other ZM analogs. However, the exposure to Fc-ZM is relatively short term (1 hour) and the binding on-rate of the Fc-ZM macromolecule to A<sub>2A</sub>R may be slower than that of the smaller ZM analogs. In addition, the concentration of Fc-ZM, which was deduced by coomassie staining of the Fc component, may overestimate the molar level of Fc-ZM relative to A-ZM, ZM, and C-ZM, which were determined by more conventional methods.

### Binding to Fc Receptors.

Next we examined the ability of Fc-ZM to bind the Fc receptors. Mouse IgG3 is known to bind to two Fc receptor isotypes: Fc $\gamma$ RI and FcRn. Fc $\gamma$ RI is typically found on dendritic cells where receptor binding leads to cell activation via the immunoreceptor tyrosine-based activation motif (ITAM)<sup>[8]</sup>. On the other hand, FcRn expression is found on most myeloid and lymphoid cell types except T cells, NK cells, and eosinophils<sup>[8]</sup>. As mentioned, FcRn is known to be responsible for uptake, transport, and recycling of antibodies. Binding to FcRn occurs at the C<sub>H</sub>2-C<sub>H</sub>3 region, independent of Fc glycosylation<sup>[16]</sup>. Unlike other Fc receptors, however, FcRn binds most Fc domains at acidic pH<sup>[8]</sup>, as present in endocytic vesicles. We therefore investigated the potential of Fc-ZM to bind both the Fc $\gamma$ RI and the FcRn at pH 7.4 and pH 6.4 via surface plasmon resonance (SPR). In order to measure the affinities at low pH, we immobilized Fc $\gamma$ RI and FcRn through amine coupling to the chips and injected Fc and Fc-ZM as analytes. As shown in Figure 4, both Fc and Fc-ZM were able to bind Fc $\gamma$ RI and FcRn at pH 6.4, with the affinity to FcRn being approximately one order of magnitude higher than Fc $\gamma$ RI. When the pH is increased from 6.4 to 7.4, affinity to Fc $\gamma$ RI increased by about 2-fold, whereas the affinity to FcRn decreased by 6- to 10-fold (Fig. S3). These data confirm that Fc-ZM retains the classical properties of antibody Fc domains to interact with these two key receptor subtypes.

### *Ex vivo* T-cell Response.

Initial characterization of Fc-ZM's immune properties was carried out in a cellular system. We treated wild-type mouse splenocytes with Fc-ZM and controls, in the presence of 0.5  $\mu$ g/ml of anti-CD3 with or without CGS inhibition for 48 hours, and measured the level of interferon  $\gamma$  (IFN $\gamma$ ) accumulated in the supernatant. As expected, A<sub>2A</sub>R activation by CGS decreased the amount of IFN $\gamma$  produced by the splenocytes whereas ZM had no effect on their IFN $\gamma$  production (Fig. 5A). Interestingly, treatment with Fc alone resulted in increased levels of IFN $\gamma$  in the supernatant, presumably through the activation of immune cells via Fc $\gamma$ R engagement. The separate addition of ZM with Fc did not further stimulate the cells, in contrast to Fc-ZM which showed enhanced activation. In fact, cells that were treated with Fc-ZM were robust producers of IFN $\gamma$ , leading to extracellular levels that were 6-fold higher than that of the untreated cells. This increase caused by Fc-ZM suggests potential strengthening of cell-cell interactions between lymphocytes and antigen-presenting cells. In addition, the increase was observable even in the presence of a high concentration of CGS (9-fold molar excess, Fig. 5B), further confirming that the ZM moiety retained its ability to bind and inhibit the A<sub>2A</sub>R.

Moreover, testing the same treatments in mouse splenocytes lacking the A<sub>2A</sub>R (Fig. 5C and 5D) or the Fc $\gamma$ Rs (Fig. 5E and 5F) diminished the immunostimulatory effect of Fc-ZM in

a fashion consistent with the proposed mechanism, suggesting that the observed phenomenon involves the  $A_{2A}R$  and the  $Fc\gamma R$ s. Overall, the observation that Fc-ZM can increase  $IFN\gamma$  production from wild-type splenocytes significantly more than either component alone serves to illustrate the benefits of using protein-small molecule conjugates as immunomodulators.

### ***In vivo* Response to Vaccinia infection.**

To examine whether the reversal of CGS effects by Fc-ZM observed *ex vivo* can be extended to an *in vivo* setting, we looked at its effects on the acute response to Vaccinia virus infection. In this model<sup>[17]</sup>, we infected wild type C57BL/6 mice with Vaccinia virus expressing ovalbumin and treated them with various drug combinations over the five days post-infection. Spleens were harvested on the sixth day post-infection and the number of total splenocytes, as an indication of systemic immune response, was quantified by counting (Fig. 6). In comparison to vehicle treatment, CGS treatment decreased the number of total splenocytes by approximately 3-fold. This inhibition was reversed by ZM when given twice daily to match the dosing schedule of CGS. When ZM was given once daily, the reversal was incomplete, suggesting that ZM is largely metabolized and/or cleared from the system by the time the second dose of CGS is administered (at least 4 hours after the first dose). By contrast, Fc-ZM, but not Fc, was able to reverse the inhibitory effects of CGS when given only two intraperitoneal injections total (day 1 and day 3 post-infection). As predicted, the ability of Fc-ZM to match ZM in reversing the immuno-inhibitory effects of CGS, even at a significantly reduced dosing frequency, is consistent with Fc-ZM's prolonged half-life resulting in extended periods of antagonism at the  $A_{2A}R$ . It is also important to note that the molar dose of Fc-ZM was 50-fold less compared to that of CGS. These results suggest that Fc-ZM, as a bivalent molecule, may have enhanced apparent potency to the  $A_{2A}R$ , potentially by engaging with multiple  $A_{2A}R$ s or with  $A_{2A}R$ s and  $FcR$ s on neighboring lymphocytes and antigen-presenting cells simultaneously.

### ***In vivo* Cardiotoxicity of Fc-small molecule conjugates.**

Notably, in the Vaccinia model described above, mice that received CGS without an antagonist appeared to be cachectic (reduced activity and impaired breathing) shortly after the first dose. Since the heart tissue is known to have high levels of  $A_{2A}R$  expression, we wondered whether the improved therapeutic profile of Fc protein-small molecule conjugates would lead to reduced cardiovascular toxicity when compared to the small molecule drug alone. To test this, we administered a previously synthesized Fc-small molecule conjugate, Fc-CGS (50 nmol/kg)<sup>[51]</sup>, along with PBS and CGS (5  $\mu$ mol/kg) into anesthetized wild-type mice and monitored their heart rate changes via an electrocardiogram (EKG) for 20 minutes (Fig. 7A). Approximately 5 minutes following the intraperitoneal injection, CGS induced tachycardia (Fig. 7B). In contrast, neither PBS nor Fc-CGS at its therapeutically appropriate

dose<sup>[5, 15]</sup> induced tachycardia in mice. It is important to note that the bolus concentration of CGS, at its therapeutic dose<sup>[15]</sup>, is predicted to be much higher than Fc-CGS, at least for the first 30 minutes after administration. This observation is consistent with the hypothesis that conjugation with Fc can enhance the pharmacologic properties of small-molecule drugs such as CGS and ZM, resulting in more efficacious and safer dosing.

## Conclusion

In this study we have designed, synthesized, and tested a novel Fc protein-small molecule conjugate, Fc-ZM, for the purpose of immune enhancement. The design strategy allowed for a controlled, site-specific conjugation between the Fc domain protein and the modified A<sub>2A</sub>R antagonist, A-ZM. Binding studies *in vitro* demonstrated the ability of Fc-ZM to bind FcRn and FcγRI, and functionally inhibit the activation of A<sub>2A</sub>R in a manner similar to its small-molecule precursor, ZM. In both *ex vivo* and *in vivo* immune response models, Fc-ZM exhibited superior pharmacology in antagonizing the A<sub>2A</sub>R when compared to ZM. These results complement prior studies that Fc conjugation can enhance the small molecule A<sub>2A</sub>R agonist CGS<sup>[5]</sup> and highlight the versatility of this semisynthetic approach. More broadly, we propose that Fc-small molecule conjugates may be particularly effective for targeting class A GPCRs. In class A GPCRs, the ligand binding pocket is in the intramembrane region of the receptor<sup>[18]</sup>, and conventional antibodies may have difficulty achieving clean agonist or antagonist activity at this location. The power and precision of small molecules to access such targets is well-documented and Fc linkage can further augment the pharmacologic properties of such compounds. In future studies, it will be interesting to explore the application of Fc-ZM to augment checkpoint inhibitors in immune surveillance of cancer.

## Experimental Section:

### Synthesis of A-ZM.

***tert*-Butyl (*E*)-3-(4-(cyanomethyl)phenyl)acrylate (2).** A mixture of 4-hydroxybenzyl cyanide (**1**, 5.00 g, 37.6 mmol) and powdered K<sub>2</sub>CO<sub>3</sub> (12.7 g, 76.6 mmol) were dissolved in *N,N*-dimethylformamide (40 mL). Then, *tert*-butyl bromoacetate (7.4 mL, 50 mmol) was dissolved in *N,N*-dimethylformamide (10 mL) and added dropwise to the reaction at room temperature. The mixture was vigorously stirred at 40 °C for 16 h resulting in the formation of a white precipitate. The reaction was allowed to cool and then poured into water (150 mL). The organic products were extracted with dichloromethane (3 x 25 mL) and the combined organic extracts were washed with water (3 x 100 mL), brine (50 mL), dried with anhydrous sodium sulfate, filtered, and concentrated *in vacuo*. The crude yellow oil was purified by column chromatography (SiO<sub>2</sub>, 10-25% EtOAc/hexanes) to yield the desired product as a slightly yellow, viscous oil (7.6 g, 81%). <sup>1</sup>H NMR (500 MHz, CDCl<sub>3</sub>): δ 1.41 (s, 9H), 3.58 (s,

2H), 4.44 (s, 2H), 6.80 (d,  $J = 8.8$  Hz, 2H), 7.15 (d,  $J = 8.8$  Hz, 2H).  $^{13}\text{C}$  NMR (125 MHz,  $\text{CDCl}_3$ ):  $\delta$  22.22, 27.59, 65.19, 81.94, 114.71, 117.85, 122.53, 128.75, 157.19, 167.34. ESI-LRMS:  $[\text{M}+\text{H}]^+ = m/z$  248.2.

**3-(Furan-2-yl)-1H-1,2,4-triazol-5-amine (4):** 2-Furonitrile (**3**, 5.0 g, 0.05 mmol) was first dissolved in 3 mL of absolute ethanol and cooled to 0 °C in an ice bath. Dry hydrogen chloride gas was then bubbled into the mixture for 5 min after which diethyl ether was added to precipitate a solid intermediate. The isolated solid was then dissolved in pyridine (30 mL) and to it was added aminoguanidine nitrate (7.4 g, 0.05 mmol) at 0 °C. The mixture was heated to reflux for 4 h after which it was cooled to RT, filtered, and the filtrate concentrated in vacuo. The resulting crude oil was placed on ice and treated with an aqueous solution of 8M  $\text{HNO}_3$  (40 mL). The newly formed precipitate was isolated by filtration and washed with cold  $\text{H}_2\text{O}$  (10 mL) and ethanol (5 mL). The nitrate salt was suspended in near boiling  $\text{H}_2\text{O}$  (30 mL) with stirring and to it was added sodium carbonate in small portions (~1.30 g). Heating was continued until solids were completely dissolved, then the solution was allowed to cool to RT and subsequently placed on ice. The resulting precipitate was isolated by filtration, washed with  $\text{H}_2\text{O}$  (3 x 5 mL), and dried to provide the title compound as a colorless prism (**4**, 2.37 g, 29%).  $^1\text{H}$  NMR (500 MHz,  $\text{DMSO}-d_6$ ):  $\delta$  6.06 (s, 2H), 6.54 (s, 1H), 6.68 (s, 1H), 7.68 (s, 1H), 12.08 (s, 1H).  $^{13}\text{C}$  NMR (125 MHz,  $\text{DMSO}-d_6$ ):  $\delta$  107.53, 111.30, 142.68, 147.68, 152.15, 157.05. ESI-LRMS:  $[\text{M}+\text{H}]^+ = m/z$  151.2.

**2-(Furan-2-yl)-5-(methylthio)-[1,2,4]triazolo[1,5-*a*][1,3,5]triazin-7-amine (5):** Compound **4** (2.18 g, 14.5 mmol) and dimethyl *N*-cyanodithioiminocarbonate (2.33 g, 16.0 mmol) were placed in a round-bottomed flask fitted with a condenser under argon. The neat mixture was heated to 170 °C for 1 h with stirring being initiated after compounds began to melt. The reaction was then cooled to RT and the resulting solid was dry loaded and chromatographed on silica (0-50% EtOAc/DCM) to yield the desired compound as a colorless solid (**5**, 1.71 g, 48%).  $^1\text{H}$  NMR (500 MHz,  $\text{DMSO}-d_6$ ):  $\delta$  2.51 (s, 3H), 6.71 (dd,  $J = 3.4$  Hz, 1.8 Hz, 1H), 7.16 (dd,  $J = 3.4$  Hz, 0.7 Hz, 1H), 7.92 (dd,  $J = 1.7$  Hz, 0.8 Hz, 1H), 8.86 (br, 2H).  $^{13}\text{C}$  NMR (125 MHz,  $\text{DMSO}-d_6$ ):  $\delta$  13.60, 112.12, 112.57, 145.25, 145.52, 149.59, 156.19, 157.20, 173.35. ESI-LRMS:  $[\text{M}+\text{H}]^+ = m/z$  249.2.

**2-(Furan-2-yl)-5-(methylsulfonyl)-[1,2,4]triazolo[1,5-*a*][1,3,5]triazin-7-amine (6):** A solution of 3-chloroperoxybenzoic acid (77% by wt., 6.58 g, 39.7 mmol) in dichloromethane (60 mL) was added to a stirred, ice-cooled suspension of compound **5** (1.5 g, 6.1 mmol) in dichloromethane (60 mL). The resulting suspension was allowed to warm to ambient temperature and stirring was continued for 16 h. The solvent was evaporated and the resulting solid triturated in ethanol (30 mL). The suspension was then cooled on ice and the precipitate

was isolated by filtration to provide the desired material as a white, crystalline solid (1.4 g, 83%).  $^1\text{H}$  NMR (500 MHz,  $\text{DMSO-}d_6$ ):  $\delta$  3.37 (s, 3H), 6.76 (dd,  $J = 3.3$  Hz, 1.7 Hz, 1H), 7.27 (d,  $J = 3.5$  Hz, 1H), 7.99 (m, 1H), 9.65 (br, 2H).  $^{13}\text{C}$  NMR (125 MHz,  $\text{DMSO-}d_6$ ):  $\delta$  38.89, 112.34, 113.42, 144.97, 145.79, 152.19, 156.84, 157.32, 165.30. ESI-LRMS:  $[\text{M}+\text{H}]^+ = m/z$  281.0.

**2-(4-(2-((7-Amino-2-(furan-2-yl)-[1,2,4]triazolo[1,5-*a*][1,3,5]triazin-5-yl)amino)ethyl)phenyl)acetic acid (A-ZM).** Compound **2** (3.80 g, 15.4 mmol) was dissolved in 100 mL of 2-propanol in a Parr shaker together with 25 mL of 1N HCl and 1 g of the 10% Pd/C catalyst. The reaction mixture was hydrogenated at 50 psi and shaken for 6 h at room temperature. The reaction was then filtered through a bed of Celite and the filter cake was washed with isopropanol (100 mL). The combined filtrate and wash were concentrated in vacuo and then partitioned between saturated aqueous sodium bicarbonate (50 mL) and diethyl ether (50 mL). The organic layer was isolated and the aqueous layer was further extracted with diethyl ether (30 mL). The combined organic extracts were dried with anhydrous sodium sulfate, filtered, and concentrated in vacuo to yield compound **7** as a colorless oil that was used without further purification. Compound **7** was then diluted in acetonitrile (5 mL) and slowly added to a solution of **6**, also dissolved in acetonitrile (5 mL). The reaction mixture was stirred for 16 h at room temperature after which the solvent was removed in vacuo and the reaction chromatographed on silica (5% MeOH/DCM) to provide a viscous yellow oil. The oil was taken up in ethyl acetate and recrystallized to yield the penultimate ester, *tert*-butyl 2-(4-(2-((7-amino-2-(furan-2-yl)-[1,2,4]triazolo[1,5-*a*][1,3,5]triazin-5-yl)amino)ethyl)phenyl)acetate, as a white solid (yield: 0.6 g, 76%).  $^1\text{H}$  NMR (500 MHz,  $\text{DMSO-}d_6$ ):  $\delta$  1.41 (s, 9H), 2.78 (m, 2H), 3.45 (m, 2H), 4.59 (s, 2H), 6.67 (s, 1H), 6.82 (d,  $J = 8.3$  Hz, 2H), 7.05 (d,  $J = 3.1$  Hz, 1H), 7.16 (d,  $J = 8.2$  Hz, 2H), 7.46 (m, 1H), 7.86 (s, 1H), 8.28 (m, 2H).  $^{13}\text{C}$  NMR (125 MHz,  $\text{DMSO-}d_6$ ):  $\delta$  27.69, 33.87, 42.36, 65.00, 81.29, 111.61, 111.90, 114.32, 129.58, 132.11, 144.61, 146.19, 150.01, 155.80, 156.06, 159.19, 161.08, 167.96. ESI-LRMS:  $[\text{M}+\text{H}]^+ = m/z$  452.2.

The *tert*-butyl ester (0.40 g, 0.89 mmol) was dissolved in a 3:1:1 mixture of tetrahydrofuran/methanol/water (20 mL) and to it was added lithium hydroxide (0.17 g, 7.1 mmol). The reaction was stirred at room temperature for 1 h after which it was complete as evidenced by TLC. Then, the mixture was acidified to pH 2 with 1N HCl and the resulting precipitate was isolated by filtration and washed with water to provide the title compound as a white solid (0.28 g, 79%).  $^1\text{H}$  NMR (500 MHz,  $\text{DMSO-}d_6$ ):  $\delta$  2.78 (t,  $J = 7.5$  Hz, 2H), 3.44 (m, 2H), 4.62 (s, 2H), 6.67 (dd,  $J = 3.3$  Hz, 1.7 Hz, 1H), 6.84 (d,  $J = 8.6$ , 2H), 7.05 (dd,  $J = 3.5$  Hz, 0.8 Hz, 1H), 7.17 (m, 2H), 7.50 (m, 1H), 7.86 (s, 1H), 8.30 (m, 2H) (Fig. S1a).  $^{13}\text{C}$  NMR (125 MHz,  $\text{DMSO-}d_6$ ):  $\delta$  33.82, 42.44, 64.48, 112.01, 112.38, 114.30, 129.59, 131.94,

144.91, 145.14, 145.53, 149.94, 156.16, 158.53, 160.99, 170.26 (Fig. S1b). ESI-HRMS: calcd. for  $C_{18}H_{18}N_7O_4$ :  $[M+H]^+ = m/z$  396.1420, found:  $[M+H]^+ = m/z$  396.1415 (Fig. S1c).

**Synthesis of C-ZM.** *tert*-Butyl (14-amino-5-oxo-1,1,1-triphenyl-9,12-dioxa-2-thia-6-azatetra decan-4-yl) carbamate (0.20 g, 0.33 mmol), synthesized as previously described<sup>[5]</sup>, was dissolved in anhydrous tetrahydrofuran (3 mL) and added to PAL resin (MidWest Bio-Tech) (0.10 g, 0.09 mmol) suspended in anhydrous THF (2 mL). Glacial acetic acid (0.10 mL) was added to this mixture and the reaction was allowed to stir at room temperature for 1 h. Then,  $NaBH(OAc)_3$  (0.16 g, 0.77 mmol) was added and stirring was continued overnight. The resin was then washed with methanol (5 x 5 mL), *N,N*-dimethylformamide (5 x 5 mL) and dichloromethane (5 x 5 mL) in a Bio-Rad Poly-Prep Chromatography Column. The subsequent coupling reactions with Fmoc-8-amino-3,6-dioxaoctanoic acid (139 mg, 0.35 mmol each reaction) and A-ZM (17.8 mg, 0.045 mmol prepared as previously described) were based on standard solid phase peptide synthesis methodology. Coupling was carried out at room temperature for 3 h with 5% diisopropylethylamine (1.8 mL) and *O*-(Benzotriazol-1-yl)-*N,N,N',N'*-tetramethyluronium hexafluorophosphate (HBTU, 133 mg, 0.35 mmol). Fluorenylmethoxycarbonyl deprotection was carried out at room temperature for 1 h with 20% piperidine (3 mL). The solvent used for both reactions was *N*-methyl-2-pyrrolidone (NMP). The crude product was cleaved from the PAL resin with 4 mL of a 95% TFA (trifluoroacetic acid), 2.5% ddH<sub>2</sub>O and 2.5% triisopropylsilane solution at room temperature for 1 hour, dried under vacuum, resuspended in 7 mL of ddH<sub>2</sub>O containing 0.05% TFA and then filtered through a 0.2  $\mu$ m filter to remove all insoluble particles. The filtrate was further purified by reverse-phase high performance liquid chromatography (HPLC), Varian Dynamax Microsorb 100-5 C18 column (250 x 21.4 mm), gradient: 5% to 60% acetonitrile/ddH<sub>2</sub>O, 50 min; 60%-100% acetonitrile/H<sub>2</sub>O, 5 min; 100% acetonitrile, 10 min; 100%-5% acetonitrile/H<sub>2</sub>O, 10 minutes; the flow rate was 10 mL per minute. The final purified product, C-ZM, was lyophilized and isolated as a fine brownish powder (16 mg, 13%). Compound characterization was done via analytical HPLC and electrospray ionization (ESI) mass spectrometry (Figure S2a and S2b).

**Synthesis of Fc-ZM.** The Fc domain of the mouse IgG3 gene (aa 104-330) was expressed and isolated as previously described<sup>[5]</sup>. Briefly, Sf9 insect cells were grown in serum-free media (Sf-900 III, Invitrogen) in suspension culture at 27 °C. Fc-intein-CBD recombinant protein was expressed and secreted by Sf9 insect cells to the supernatant, which was collected by centrifugation at 1,500 rpm for 10 min and filtered through a 0.2  $\mu$ m filter to remove the cell pellet and debris. The Fc-intein-CBD fusion protein was then purified by passing the supernatant over a bed of chitin beads (NEB, 2 mL bed volume per liter culture) by gravity flow. The beads were washed with 50 mL of phosphate buffered saline (PBS) 5 times before

being subjected to ligation with C-ZM. To initiate the ligation with C-ZM, 1-2 column volumes of 400 mM sodium 2-mercaptoethanesulfonate in PBS (pH = 7.4) containing more than 100 molar equivalents of C-ZM was added to the column. The column was purged with argon and the reaction was carried out at room temperature over 72 h. The ligated product was eluted from the column with 5 x 1 column volume of PBS, and the combined elutions were dialyzed against 4 L of PBS using a 10 kDa molecular weight cutoff (MWCO) dialysis cassette (Slide-A-Lyzer™, Thermo Fisher Scientific). Each buffer exchange lasted at least 6 h, with a total of six buffer exchanges. The final Fc-ZM was further concentrated to 0.5-1 mg/mL and stored at -80 °C. Purified yields were in the range of 0.5 to 1 mg Fc-ZM per liter of Sf9 cell culture.

**Liquid Chromatography Mass Spectrometry (LC-MS) analysis of Fc-ZM.** LC-MS was performed on a LXQ system (Thermo Scientific) with a Poroshell 300SB-C8 column (5 µm, 75 x 1.0 mm). Fc-ZM was first digested with PNGase F (New England Biolabs) according to the protocol provided by the manufacturer. The digested sample was then treated with 50 mM DTT and heated at 55 °C for 20 min before subjecting it to LC-MS analysis. The LC was performed at 60 °C eluting with a linear gradient of 20-40% acetonitrile/water containing 0.1% formic acid over 10 min at a flow rate of 0.25 mL/min.

**Intracellular cAMP (cyclic AMP) measurements via enzyme-linked immunosorbent assay.** Splens from wild type (C57BL/6) mice were harvested and crushed on a cell strainer (BD Bioscience). The red blood cells were then removed using ACK lysis buffer. The isolated splenocytes were seeded in 96-well plates with AE7 medium (45% RPMI 1640, 45% EHAA Clicks, 10% fetal bovine serum, 1% antibiotics, 1% L-Glutamine, 0.1% Gentamycin, 0.05% 2-mercaptoethanol) and activated by 2 µg/mL of soluble anti-CD3 and anti-CD28 for 48 h, then rested in fresh medium without anti-CD3 or anti-CD28 for 24 h before drug treatments. To determine the effects of CGS, ZM, A-ZM, C-ZM, Fc, and Fc-ZM on A<sub>2A</sub>R function, the amount of total cAMP produced in wild type (C57BL/6) splenocytes was assayed with the cAMP Biotrak EIA system (GE Healthcare Life Science) according to the manufacturer's instructions. Stock concentrations of A-ZM, C-ZM, and Fc-ZM were determined by dry weight, UV absorbance (at 260 nm), and Coomassie staining, respectively.

**Surface Plasmon Resonance (SPR) Measurements.** SPR measurements were performed on a Biacore T200 instrument (GE Healthcare). FcRn and FcγRI were immobilized in different channels on a CM5 sensor chip (GE Healthcare) using an amine coupling kit following methods provided by the manufacturer. The sensor chip surface was activated with NHS and EDC followed by flowing of receptors until 2000 resonance units (RU) were obtained. A blank reference cell was used as a reference. Fc and drug conjugated Fc (Fc-ZM) were flown

over the cell as analytes. HBS-P+ buffer (10 mM HEPES, 150 mM NaCl, 0.05% surfactant P20, pH 7.4 or 6.4) were used as sample buffer and running buffer. Association of analytes Fc and Fc-ZM were measured for three minutes with a flow rate of 20  $\mu\text{L}/\text{min}$  and allowed to dissociate for another three minutes. The surface regeneration was achieved with 3 M  $\text{MgCl}_2$  at a flow rate of 20  $\mu\text{L}/\text{min}$  for 60 s. The analytes were injected in a series of two-fold dilutions from the highest concentration used (2  $\mu\text{M}$ , 1  $\mu\text{M}$ , 500 nM, 250 nM, 125 nM, 62.5 nM, and 31.25 nM etc and blanks). Multiple individual experiments were carried out and a typical curve is presented in the figures. All sensorgrams were reference channel and blank subtracted for analyses. Kinetics data were obtained by global fitting of the binding data to a 1:1 steady state affinity of Langmuir binding model using BIAcore T200 evaluation software (GE healthcare).

**Mice.** Mice between six- to twelve-weeks of age, including both males and females, were used for all the experiments in this study. All mouse procedures were approved by the Johns Hopkins University Institutional Animal Care and Use Committee. Anesthesia was achieved using isoflurane in a closed chamber. Mice were euthanized via cervical dislocation. C57BL/6 mice were obtained from the Jackson Laboratory.  $A_{2A}R$  knock-out mice were bred and housed in pathogen-free conditions on the Johns Hopkins School of Medicine East Baltimore campus. Mice deficient of the  $\gamma$ -chain subunit of  $\text{Fc}\gamma\text{R1}$ ,  $\text{Fc}\gamma\text{RIII}$ , and  $\text{Fc}\epsilon\text{RI}$  were purchased from Taconic Biosciences (Model 583).

**Ex vivo T cell response via Interferon  $\gamma$  ELISA.** Splenocytes from wild type (C57BL/6) mice,  $A_{2A}R$  knock-out mice, and mice deficient of the  $\gamma$ -chain subunit of  $\text{Fc}\gamma\text{R1}$ ,  $\text{Fc}\gamma\text{RIII}$ , and  $\text{Fc}\epsilon\text{RI}$  (Model 583, Taconic) were isolated and cultured in round-bottom 96-well plates with AE7 medium (45% RPMI 1640, 45% EHAA Clicks, 10% fetal bovine serum, 1% antibiotics, 1% L-glutamine, 0.1% gentamycin, 0.05% 2-mercaptoethanol) over 48 h, in the presence of 0.5  $\mu\text{g}/\text{ml}$  of anti-CD3 and various drug treatments. Supernatants were harvested and the level of  $\text{IFN}\gamma$  was determined via enzyme-linked immunosorbent assay (Mouse  $\text{IFN}\gamma$  ELISA Ready-SET-Go!®, Affymetrix eBioscience).

**In vivo response to Vaccinia virus infection.** Wild type (C57BL/6) mice were infected with Vaccinia virus expressing ovalbumin on day 1 via retro-orbital injections at 1 million plaque-forming unit (PFU) per mouse. Throughout days 2 to 6, various treatments were given via intraperitoneal injections, including vehicle (20% DMSO in PBS), CGS (5.0  $\mu\text{mol}/\text{kg}$ , b.i.d.), CGS (5.0  $\mu\text{mol}/\text{kg}$ , b.i.d.) and ZM (8.9  $\mu\text{mol}/\text{kg}$ , q.d.), CGS (5.0  $\mu\text{mol}/\text{kg}$ , b.i.d.) and ZM (8.9  $\mu\text{mol}/\text{kg}$ , b.i.d.), CGS (5.0  $\mu\text{mol}/\text{kg}$ , b.i.d.) and Fc (100 nmol/kg, on days 2 and 4), CGS (5.0  $\mu\text{mol}/\text{kg}$ , b.i.d.) and Fc-ZM (100 nmol/kg, on days 2 and 4). Importantly, Fc and Fc-ZM was given one hour before CGS injections. On day 7, splenocytes were harvested and

counted using a hemocytometer.

**Statistical analysis.** All graphs were created using GraphPad Prism software, and statistical analysis was performed with GraphPad Prism. Comparisons between three or more independent groups were assessed by one-way ANOVA with a Tukey's multiple-comparisons test.

***In vivo* cardiovascular response to CGS and Fc-CGS.** Wild type (C57BL/6) mice were anesthetized with 3% isoflurane and maintained under 2% isoflurane anesthesia throughout EKG acquisition. Anesthetized mice were placed in a supine position on a temperature controlled heating pad. Body temperature was monitored with rectal probe and maintained at 37–38°C. EKG probes were inserted subcutaneously and EKG signal (Standard lead II) was obtained using a PowerLab data acquisition system (ML866) and Animal Bio Amp (ML136; AD Instruments, Colorado Springs, CO, USA). Vehicle (PBS), 5 µmol/kg of CGS, or 50 nmol/kg of Fc-CGS was administered via intraperitoneal injections. 5 min of EKG signal were recorded prior to each injection, followed by 20 min of recording after the injection. LabChart Pro 7.2 software (AD Instruments, Colorado Springs, CO, USA) was used for automated EKG tracing analysis.

#### **Acknowledgements:**

This work was supported by the National Institutes of Health and the FAMRI Foundation. We thank Dr. Yana Li (The Eukaryotic Tissue Culture Facility at Johns Hopkins) for her help and support with insect cell culture. We thank Safiat Ayinde (Department of Pharmacology and Molecular Sciences, Johns Hopkins School of Medicine) for her help with peptide synthesis and protein expression. We also thank Dr. Robert Leone, Chirag Patel, Min-Hee Oh and Jiayu Wen (Department of Oncology, Johns Hopkins School of Medicine) for their guidance and training in immunology research and animal care.

#### **References:**

- [1] B. B. Fredholm, I. J. AP, K. A. Jacobson, K. N. Klotz, J. Linden, *Pharmacol Rev* **2001**, *53*, 527-552.
- [2] M. de Lera Ruiz, Y. H. Lim, J. Zheng, *Journal of medicinal chemistry* **2014**, *57*, 3623-3650.
- [3] aA. Ohta, E. Gorelik, S. J. Prasad, F. Ronchese, D. Lukashev, M. K. Wong, X. Huang, S. Caldwell, K. Liu, P. Smith, J. F. Chen, E. K. Jackson, S. Apasov, S. Abrams, M. Sitkovsky, *Proc Natl Acad Sci U S A* **2006**, *103*, 13132-13137; bO. P. Dall'Igna, L. O. Porciuncula, D. O. Souza, R. A. Cunha, D. R. Lara, *British journal of pharmacology* **2003**, *138*, 1207-1209; cK. Golembiowska, A. Dziubina, *Neuropharmacology* **2004**, *47*, 414-426.

- [4] J. P. Chovan, P. A. Zane, G. E. Greenberg, *Journal of chromatography* **1992**, *578*, 77-83.
- [5] M. J. Chiang, M. A. Holbert, J. H. Kalin, Y. H. Ahn, J. Giddens, M. N. Amin, M. S. Taylor, S. L. Collins, Y. Chan-Li, A. Waickman, P. Y. Hsiao, D. Bolduc, D. J. Leahy, M. R. Horton, L. X. Wang, J. D. Powell, P. A. Cole, *Journal of the American Chemical Society* **2014**, *136*, 3370-3373.
- [6] D. Levin, B. Golding, S. E. Strome, Z. E. Sauna, *Trends in biotechnology* **2015**, *33*, 27-34.
- [7] aD. M. Czajkowsky, J. Hu, Z. Shao, R. J. Pleass, *EMBO molecular medicine* **2012**, *4*, 1015-1028; bS. Mitragotri, P. A. Burke, R. Langer, *Nature reviews. Drug discovery* **2014**, *13*, 655-672.
- [8] P. Bruhns, *Blood* **2012**, *119*, 5640-5649.
- [9] K. Peppel, D. Crawford, B. Beutler, *The Journal of experimental medicine* **1991**, *174*, 1483-1489.
- [10] T. W. Muir, D. Sondhi, P. A. Cole, *Proc Natl Acad Sci U S A* **1998**, *95*, 6705-6710.
- [11] aS. M. Poucher, J. R. Keddie, P. Singh, S. M. Stoggall, P. W. Caulkett, G. Jones, M. G. Coll, *British journal of pharmacology* **1995**, *115*, 1096-1102; bS. M. Poucher, J. R. Keddie, R. Brooks, G. R. Shaw, D. McKillop, *The Journal of pharmacy and pharmacology* **1996**, *48*, 601-606.
- [12] V. P. Jaakola, M. T. Griffith, M. A. Hanson, V. Cherezov, E. Y. Chien, J. R. Lane, A. P. Ijzerman, R. C. Stevens, *Science* **2008**, *322*, 1211-1217.
- [13] aP. W. R. Caulkett, G. Jones, M. McPartlin, N. D. Renshaw, S. K. Stewart, B. Wright, *Journal of the Chemical Society, Perkin Transactions 1* **1995**, 801-808; bA. J. Hutchison, M. Williams, R. de Jesus, R. Yokoyama, H. H. Oei, G. R. Ghai, R. L. Webb, H. C. Zoganas, G. A. Stone, M. F. Jarvis, *Journal of medicinal chemistry* **1990**, *33*, 1919-1924; cP. W. R. Caulkett, G. Jones, M. G. Collis, S. M. Poucher, Google Patents, **1991**.
- [14] D. Bolduc, M. Rahdar, B. Tu-Sekine, S. C. Sivakumaren, D. Raben, L. M. Amzel, P. Devreotes, S. B. Gabelli, P. Cole, *eLife* **2013**, *2*, e00691.
- [15] P. E. Zarek, C. T. Huang, E. R. Lutz, J. Kowalski, M. R. Horton, J. Linden, C. G. Drake, J. D. Powell, *Blood* **2008**, *111*, 251-259.
- [16] aW. L. Martin, P. J. Bjorkman, *Biochemistry* **1999**, *38*, 12639-12647; bV. Irani, A. J. Guy, D. Andrew, J. G. Beeson, P. A. Ramsland, J. S. Richards, *Molecular immunology* **2015**, *67*, 171-182.
- [17] K. N. Pollizzi, C. H. Patel, I. H. Sun, M. H. Oh, A. T. Waickman, J. Wen, G. M. Delgoffe, J. D. Powell, *J Clin Invest* **2015**, *125*, 2090-2108.
- [18] D. Zhang, Q. Zhao, B. Wu, *Molecules and cells* **2015**, *38*, 836-842.

## Figure Legends

**Scheme 1.** Synthesis of A-ZM. A-ZM was made from two separate building blocks, intermediates **2** and **6**. (A) The synthetic approach to intermediate **2**. (B) The synthetic route for making intermediate **6**. (C) Converting **2** and **6** into A-ZM.

**Scheme 2.** Synthesis of C-ZM. A-ZM was attached to an ethylene-oxy linker terminating in a Cys residue, which was generated via solid-phase peptide synthesis (SPPS) techniques. SPPS conditions include: (a) coupling: Fmoc-NH-(PEG)-COOH, HBTU, 5% DIPEA, NMP, RT, 3 h, and (b) deprotection: 20% piperidine, NMP, RT, 1 h.

**Figure 1.** Semisynthesis of Fc-ZM by expressed protein ligation. HBM: honeybee melittin secretion signal. CBD: chitin binding domain.

**Figure 2.** Characterization of purified Fc and Fc-ZM. (A) Fc and Fc-ZM stained with Coomassie blue after being resolved by 10% SDS-PAGE. (B) Liquid chromatography mass spectrometry (LC-MS) spectrum confirming the expected mass of Fc-ZM deglycosylated using PNGase F. Fc-ZM calculated  $m/z$  31163. The experimental error on this measurement is estimated to be  $\pm 20$  mass units.

**Figure 3.** Assessment of  $A_{2A}R$  binding via intracellular cAMP assay. Wild-type mouse splenocytes were pre-activated with 2  $\mu\text{g}/\text{mL}$  of soluble anti-CD3 and anti-CD28 for 48 h, followed by a 24 h resting period in fresh media without anti-CD3 and anti-CD28 before subjecting to drug treatments. (A) Intracellular cAMP produced after 1 h incubation in media containing various drugs at 1  $\mu\text{M}$ . (B) Intracellular cAMP produced by splenocytes treated with various drugs at 1  $\mu\text{M}$  in the presence of 1  $\mu\text{M}$  CGS. (C) Intracellular cAMP produced by splenocytes treated with various drugs at 250 nM in the presence of 1  $\mu\text{M}$  CGS. Results were analyzed using one-way ANOVA test (\*\*\*\*,  $P < 0.0001$ ) followed by a Tukey's multiple comparisons test (\*\*\*\*,  $P < 0.0001$ ).

**Figure 4.** Assessment of FcRn and Fc $\gamma$ RI Binding via surface plasmon resonance at pH 6.4. (A) and (B) shows the binding of Fc and Fc-ZM, respectively, to the immobilized mouse neonatal Fc receptor (FcRn). (C) and (D) shows the binding of Fc and Fc-ZM, respectively, to the immobilized mouse Fc $\gamma$ R1.

**Figure 5.** *Ex vivo* T-cell response via interferon  $\gamma$  ELISA. (A), (C), and (E) shows the level of IFN $\gamma$  secreted by splenocytes harvested from wild-type mice,  $A_{2A}R$  knock-out mice, and Fc $\gamma$ R1 knock-out mice (mice lacking the  $\gamma$ -chain subunit of Fc $\gamma$ R1, Fc $\gamma$ RIII, and Fc $\epsilon$ RI), respectively, following a 48 h incubation with various drug treatments at 111 nM, in the presence of 0.5  $\mu\text{g}/\text{ml}$  of anti-CD3. (B), (D), and (F) shows the level of IFN $\gamma$  secreted by

splenocytes harvested from wild-type mice, A<sub>2A</sub>R knock-out mice, and FcγR1 knock-out mice (mice lacking the γ-chain subunit of FcγR1, FcγRIII, and FcεRI), respectively, following a 48 h incubation with various drug treatments at 111 nM, in the presence of 0.5 μg/ml of anti-CD3 and 1 μM CGS. Results were analyzed by one-way ANOVA followed by a Tukey's multiple comparisons test (\*, P < 0.05; \*\*, P < 0.01; \*\*\*, P < 0.001; \*\*\*\*, P < 0.0001).

**Figure 6.** *In vivo* response to Vaccinia virus infection. Number of total splenocytes was quantified in spleens collected from mice treated with vehicle (n = 19), CGS (n = 14), CGS + ZM q.d. (n = 8), CGS + ZM b.i.d. (n = 12), CGS + Fc (n = 10), or CGS + Fc-ZM (n = 8). The results were normalized to the vehicle treatment and statistical significance determined by one-way ANOVA (P < 0.0001) followed by a Tukey's multiple comparisons test (\*, P < 0.05; \*\*, P < 0.01; \*\*\*, P < 0.001; \*\*\*\*, P < 0.0001).

**Figure 7.** *In vivo* cardiovascular response to CGS and Fc-CGS. (A) Average heart rate of mice treated with PBS (n = 3), CGS (n = 4), or Fc-CGS (n = 3), monitored over 20 minutes post-administration of the treatments. Dashed line indicates the timing of the drug injections. (B) Average heart rate at 5.5 minutes following the injection. Results were analyzed using one-way ANOVA (\*\*\*, P = 0.0002) followed by a Tukey's multiple comparisons test (\*\*\*, P < 0.001). BPM, beats per minute.

### Text Suggestion for the Table of Contents

Using a semisynthetic approach, an Fc-small molecule conjugate, Fc-ZM, was made for the targeted inhibition of the adenosine 2A receptor. Fc-ZM displayed superior pharmacologic properties compared to the small-molecule precursor ZM and was able to functionally interact with both A<sub>2A</sub>R and FcRs, present on lymphocytes and antigen-presenting cells, respectively.

Figure 1. Semisynthesis of Fc-ZM by expressed protein ligation.

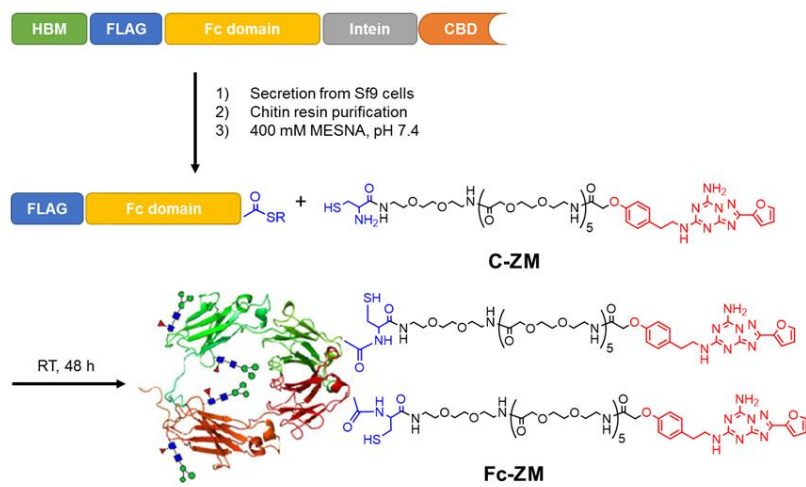


Figure 1

Figure 2. Characterization of purified Fc and Fc-ZM.

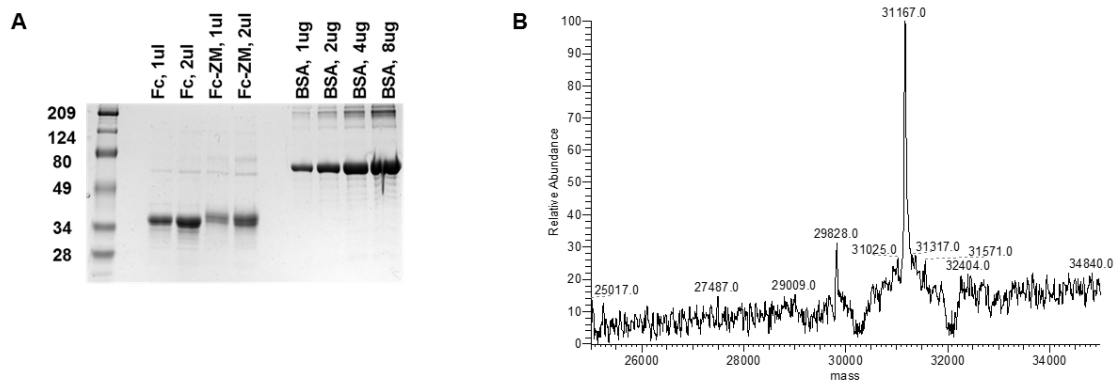


Figure 2

Figure 3. Assessment of A2AR binding via intracellular cAMP assay.

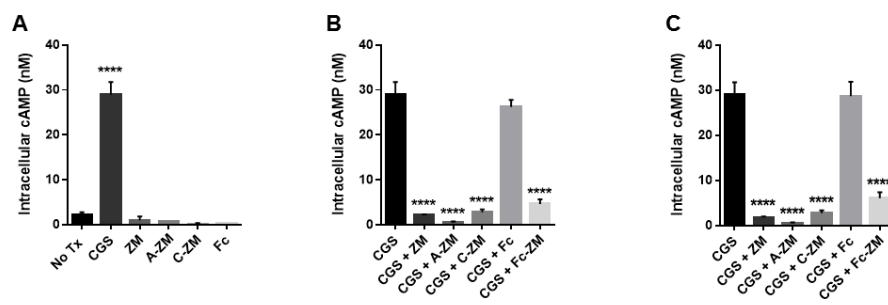


Figure 3

Figure 4. Assessment of FcRn and FcγRI Binding via surface plasmon resonance at pH 6.4.

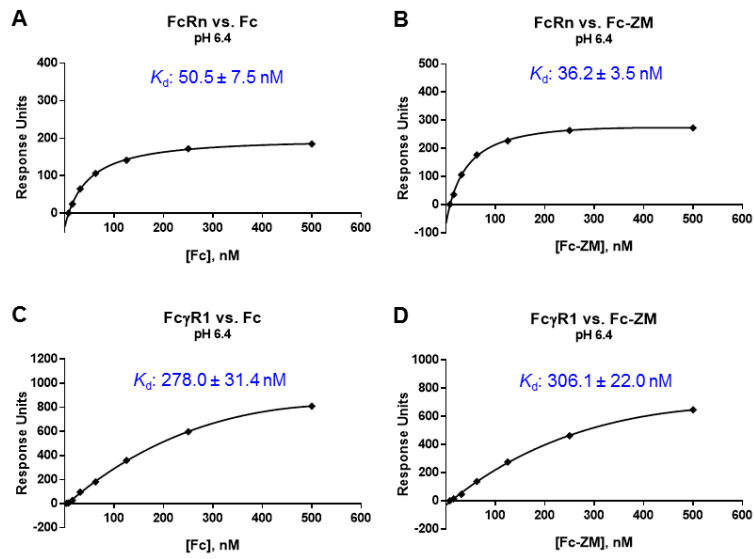


Figure 4

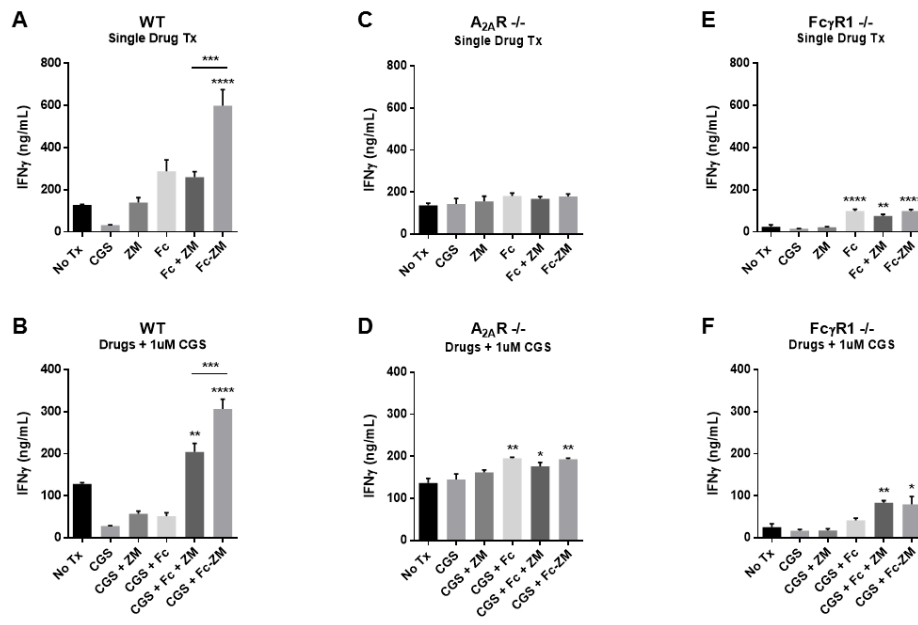
Figure 5. Ex vivo T-cell response via interferon  $\gamma$  ELISA.

Figure 5

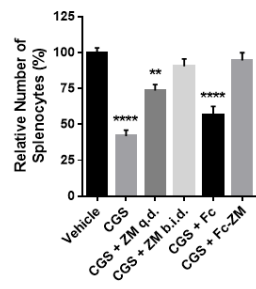
Figure 6. *In vivo* response to Vaccinia virus infection.

Figure 6

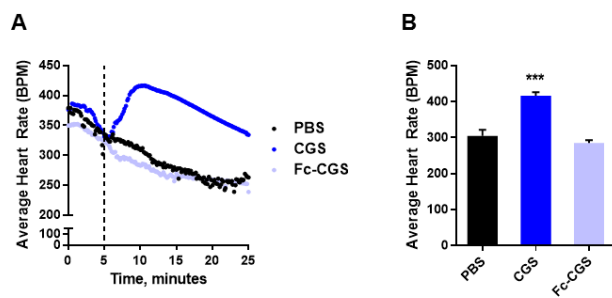
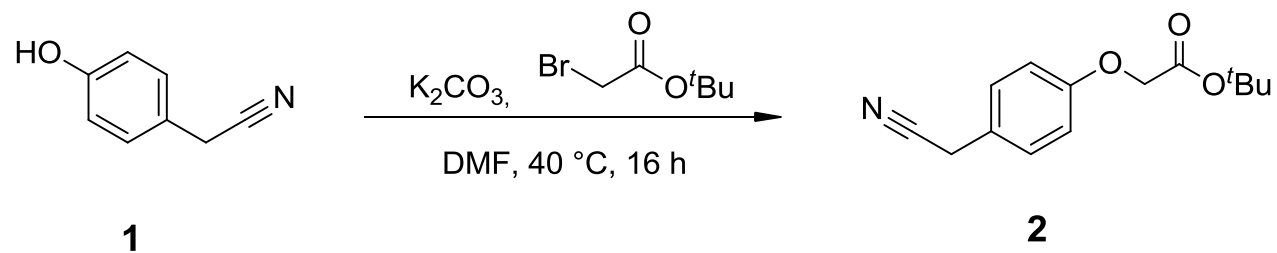
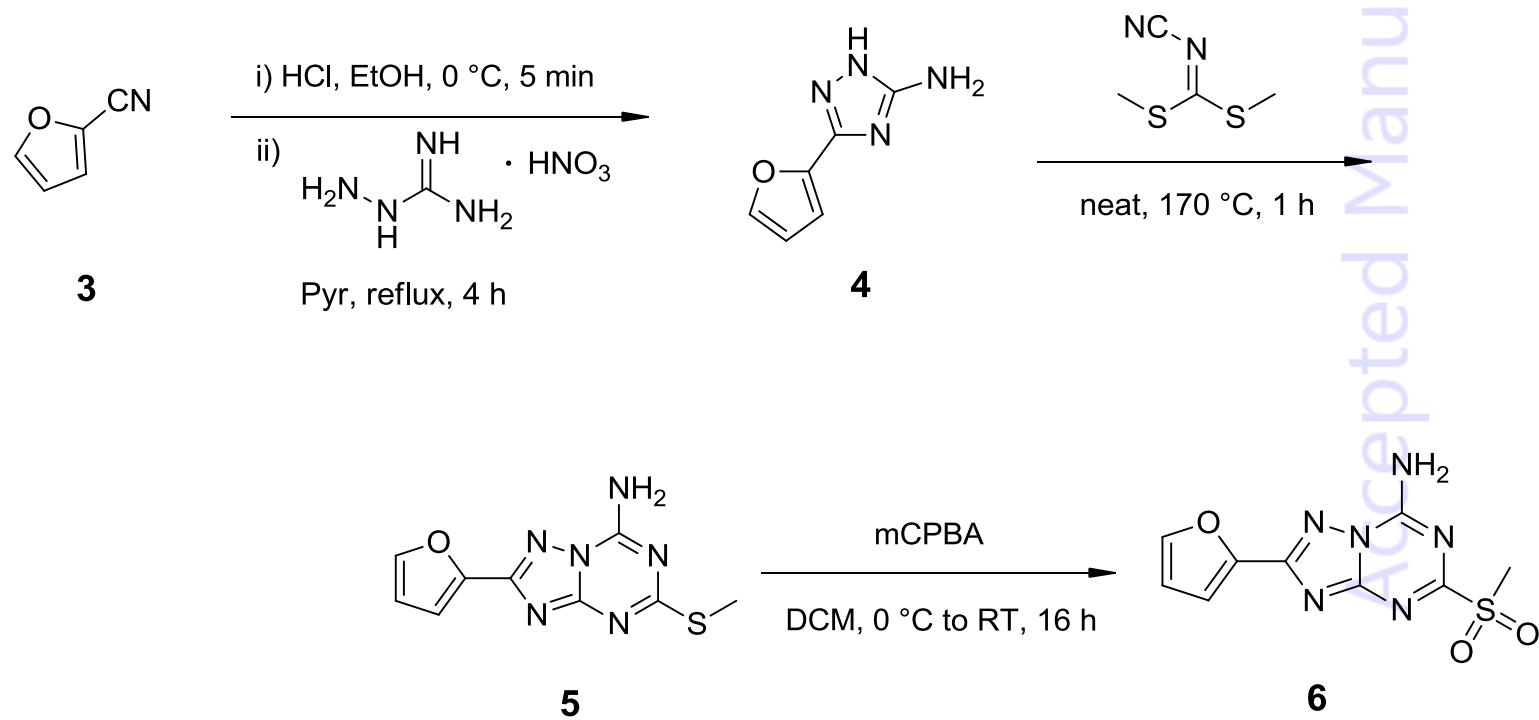
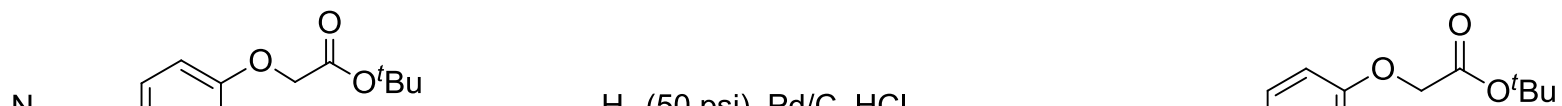
Figure 7. *In vivo* cardiovascular response to CGS and Fc-CGS.

Figure 7

Accepted Manuscript

**A****B****C**

Scheme 1

Accepted Manuscript



Scheme2

Accepted Manuscript